

## Role of Saturated Solutions of Chiral Amino Acids in Synthesis and Phase Segregation within Optically Active Polyaniline

Sudha,<sup>1</sup> Kumar Devendra,<sup>1</sup> Iwamoto Mitsumasa<sup>2</sup>

<sup>1</sup>Department of Applied Chemistry and Polymer Technology, Delhi Technological University (Formerly Delhi College of Engineering), Shahbad Daultpur, Delhi 110042, India

<sup>2</sup>Department of Physical Electronics, Tokyo Institute of Technology, 2-12-1 O-okayama, Meguro-ku, Tokyo 152-8552, Japan

Correspondence to: K. Devendra (E-mail: dkumar@dce.ac.in)

**ABSTRACT:** The saturated solutions of chiral amino acids as soft template have been shown to function as a platform for induction of optical activity through free radical polymerization reaction. The conductivity of optically active polyaniline changes with the variation in acidity of reaction medium and morphology of the material. Ultraviolet-visible and circular dichroism spectra along with scanning electron microscopy and transmission electron microscopy micrographs evaluate discrete morphologies of polymers at different pH with phase segregation between unprotonated and fully protonated domains. Four probe method shows that the branched structure caused by the presence of phenazine units in polymer chain stabilizes different charge states in polymer with higher conductivity having higher dissymmetric *g*-factor. © 2012 Wiley Periodicals, Inc. *J. Appl. Polym. Sci.* 000: 000–000, 2012

**KEYWORDS:** conducting polymer; chirality; nanostructures; phase-segregation; dissymmetric *g*-factor

Received 20 February 2012; accepted 29 April 2012; published online

DOI: 10.1002/app.37976

### INTRODUCTION

The architecture of conducting polymer-based nanostructures has become a topic of increasing interest due to their potential applications in electrical, optical, and electronics including sensor devices.<sup>1</sup> Synthesizing polyaniline (PANI) with specific morphologies has attracted much attention of researchers because it gives different physical and chemical properties from the bulk counterparts. Moreover, PANI with specific morphologies can be applied in various fields, such as chemical and bio-sensors, controlled release and delivery of drugs, light emitting and electronic devices, etc.<sup>2,3</sup> Moreover, it is also well documented that various conjugated polymers and oligomers can self-assemble into supra-molecular structures both in solution and at interfaces.<sup>4</sup> The different self-assembled structures of chiral PANI are formed by comproportionation reaction of the bipolaron and the neighboring neutral chiral polymer segments.<sup>5</sup> Various methods have been developed for the construction of these novel structures for enantioselective synthesis, asymmetric autocatalysis, autoinduction, and transformation. Introduction of a bulky substituent to a vinyl polymer or an optically active substituent to the polymer side chain, and hence, the induction of chiroptical properties have been studied extensively.<sup>6</sup> However, chiral PANI almost features one-dimensional morphology in

strong acid solution.<sup>7</sup> It is also known that amino acids are the natural chiral matters and have extra functional groups such as  $-\text{COOH}$ ,  $-\text{NH}_2$ , or heterocyclic groups. The  $-\text{COOH}$  group in the amino acids may act as the doping function to conduct polymers by hydrogen bonding. As the amino acids have both  $-\text{COOH}$  and  $-\text{NH}_2$  groups, the pH value of the amino acids solution differs from the numbers of these two groups. The pH value influences the morphology of PANI greatly<sup>8,9</sup> during polymerization. Therefore, chiral amino acids may endow chirality to PANI and control the morphology of PANI due to the change in pH value during polymerization.

Recently, we have developed a new method to transcribe various organic superstructures by chiral amino acids. The driving force in this type of reaction is considered to be electrostatic interaction, orientation of amino acid for active attack, and hydrogen bonding between amino acid and PANI chain. Herein, chiral conducting PANI was prepared with varying conductivity and discrete morphologies (i.e., flakes, flower, and fibers forms).

### EXPERIMENTS

#### Materials

The naturally occurring chiral amino acids such as L-leucine (L-Leu), L-isoleucine (L-Ile), and L-phenylalanine (L-Phe) were

Additional Supporting Information may be found in the online version of this article.

© 2012 Wiley Periodicals, Inc.

purchased from Spectrochem Pvt. Ltd., Mumbai, India. Ammonium persulphate (APS) and aniline were procured from Merck Specialties Pvt. Ltd., Mumbai, India, while chloroform from Sisco Research Pvt., Mumbai, India. All reagents were of analytical grade. Aniline was double distilled and stored at low temperature before its use. Other chemicals were used as received without further purification. Double distilled and demineralized water from Millipore (Millipore (India) Pvt. Ltd., Bangalore, India) was used throughout the studies.

### Synthesis of Chiral PANI

The chiral PANI has been synthesized through soft template method using different naturally occurring buffer solutions of chiral amino acids such as L-leucine (L-Leu), L-isoleucine (L-Ile), and L-phenylalanine (L-Phe). An appropriate amount of aniline was dissolved in 5 mL of buffer solution of amino acids at 0–5°C, and 5 mL 0.1M APS solution was added dropwise into the above solution. This reaction mixture was stirred vigorously for 10 min and kept in a static state for 24 h at 0–5°C. The precipitate so obtained was filtered, rinsed by deionized water and acetone several times, and dried in vacuum at 60°C overnight. Finally, brown PANI powder was obtained. Similarly, other PANI samples were also prepared by using the same method except a change in concentration of APS, i.e., 0.05M APS instead of 0.1M APS solution for the synthesis of chiral PANI.

### Characterization

Ultraviolet-visible (UV-vis) spectra of all the samples were recorded using a double beam UV-vis spectrophotometer (Model UV5704SS) ECIL, India, over the range of 200–700 nm. Fourier transform infrared (FTIR) spectra of these samples were recorded in transmission mode with KBr pressed pellets using a Perkin-Elmer (Model No. 2000, UK) spectrometer. Circular dichroism (CD) spectra of the solutions were recorded at chira-scan circular dichromator. The powder X-ray diffraction patterns of the samples were recorded on Rigaku miniflex diffractometer using  $\text{CuK}_{\alpha 1}$  radiation at a scan rate of  $1^\circ \text{ min}^{-1}$  and step size  $0.02^\circ$  from  $2\theta$  range  $5^\circ$ – $60^\circ$ . The morphology of samples was also studied by using electron microscope (Hitachi scanning electron microscope, Model S-3700N) at an acceleration voltage of 10 kV. All samples were plasma coated with a thin layer of gold to provide electrical conduction and reduce surface charging. The evaluation of morphologies were done on a high-resolution transmission electron microscopy (HRTEM) (Philips Tecnai G<sup>2</sup> 30 transmission electron microscope with 300 kV accelerating voltage).

## RESULTS AND DISCUSSION

The synthesized PANI samples were found to be amorphous in nature with less crystallinity, which show diffuse broad peak ranging from  $10^\circ$  to  $23^\circ$  as depicted in Supporting Information Figure S1, and this pattern is similar to the work reported earlier.<sup>10</sup> The morphology of synthesized PANI samples have been reported in Figure 1 by using electron microscopy. It is noticed that when the concentration of APS was taken as 0.1M, the synthesized PANI is fibrous in nature, whose diameter is in the range of 10–30 nm. The scanning electron microscopy (SEM)

micrographs are shown in Figure 1(a–c) and insets show SEM micrographs at higher magnification and HRTEM images. Furthermore, when the initiator (APS) concentration was taken as 0.05M, most of the synthesized PANI is of flaky morphology with smooth surface, and these flakes stake together as flowers or other discrete structures. The thickness and lateral dimensions of these flakes are in the range of 20–50 nm and 1–2  $\mu\text{m}$ , respectively, as shown in Figure 1(d–f). It is possible that the chiral PANI with discrete morphologies can also be conducting because of the conducting nature of PANI salt. To establish this fact, the DC conductivity has been measured by using four-point probe method, and data are tabulated in Table I. The conductivity data revealed that when the molar ratio of APS is low, the conductivity is high but with the increase in molar ratio the conductivity of chiral PANI decreases, but it is higher than achiral PANI salt.

Mechanism behind different types of interactions which are responsible for discrete morphologies is further studied using FTIR, UV-vis, and CD spectroscopies and pH of media. Figure 2 shows the FTIR spectra of typical chiral PANI prepared from naturally occurring amino acids. The bands at 860 and 760  $\text{cm}^{-1}$  present the branching polymer chains with tri- and tetrasubstituted aromatic rings in emeraldine form. However, 1,2,4-tri- or 1,2,4,5-tetrasubstituted benzene rings can also be associated with the 2- or 2,3-substituted phenazine units in the polymer structure, respectively.<sup>11</sup> It is revealed from the data that 1450  $\text{cm}^{-1}$  band corresponds to the ring stretching mode of phenazine units,<sup>12</sup> and the peak at 1415  $\text{cm}^{-1}$  is associated with phenazine-like units in the structure of PANI.<sup>13</sup> The spectrum of phenazine has a strong skeletal and a C–H in-plane deformation band in the region at 1215–1170 and 911  $\text{cm}^{-1}$ , both of which are visible in the spectra of L-Leu and L-Phe doped PANI polymers. A broad band at 1800–3000  $\text{cm}^{-1}$  is typical for conducting form of PANI and attributed to  $\pi$ -electron delocalization in the polaron structure of doped PANI.<sup>14</sup> The characteristic peaks at 1504 and 1576  $\text{cm}^{-1}$  are ascribed to the C–C stretching vibration of benzenoid and quinoid rings, respectively. The peak at 1289  $\text{cm}^{-1}$  is attributed to the C–N stretching of the secondary aromatic amine. The peaks at 1170 and 842  $\text{cm}^{-1}$  are generated from the C–H in-plane bending and out-of-plane bending, respectively.

In addition to the characteristic peaks mentioned earlier, the peaks at 1036 and 507  $\text{cm}^{-1}$  correspond to the absorption of the –COOH group, indicating that the resulting PANI is bonded by amino acids. The peak at 1130  $\text{cm}^{-1}$ , related to the doped structure, has shifted to lower frequency with change in structural motifs of chiral amino acid. It signifies that the chiral PANI synthesized from aromatic amino acid is more protonated than the linear one, leading to a higher conductivity. The intensive peaks at 3274 and 3205  $\text{cm}^{-1}$  are caused by the different types of intra- and intermolecular hydrogen bonded N–H stretching vibration of secondary amines as suggested in earlier study.<sup>15</sup> The peak at 3056  $\text{cm}^{-1}$  is the C–H stretching on aromatic ring of PANI. Furthermore, the hydrogen bonding intensifies with the decrease in pH of the medium, which is suggested by the slight shift of these peaks to the lower wavelength and sharpness of the peak. Intensified hydrogen bonding is important in the formation of self-assembled supramolecular structures, especially flaky morphology.

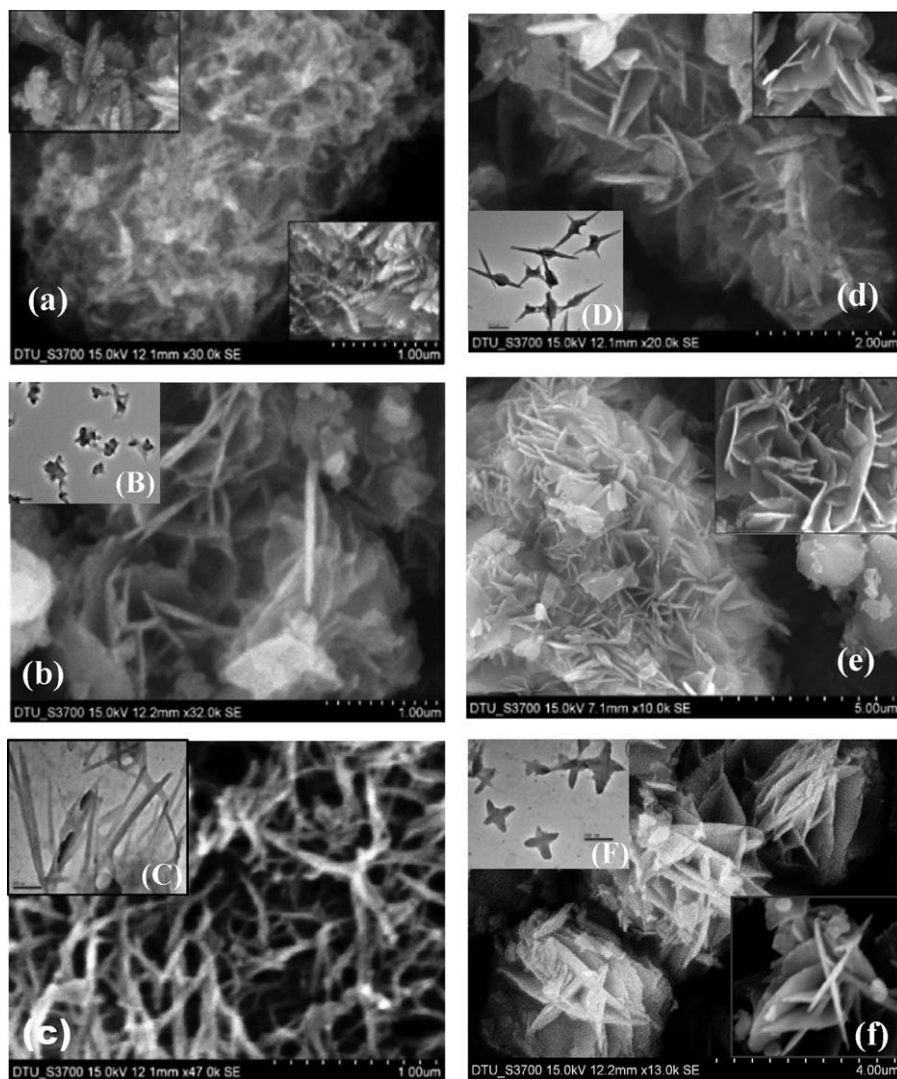


**Figure 1.** SEM micrographs of chiral PANI at 0.1M APS for (a) L-Ile.PANI, (b) L-Leu.PANI, and (c) L-Phe.PANI; and at 0.05M APS for (d) L-Ile.PANI, (e) L-Leu.PANI, and (f) L-Phe.PANI. Insets show SEM micrographs at higher magnification, while B, C, D, and F represent their respective HRTEM micrographs.

To analyze the growth mechanism (as shown in Supporting Information Figure S2) of these specific morphologies, the evolution of pH value of the reaction mixture with time was measured, and it is represented in Figure 3. In all cases, the initial pH of saturated amino acids with aniline was in the range of 5–5.5. The pH value of the reaction mixture decreased immedi-

ately after adding APS due to the production of sulfuric acid during the polymerization.<sup>16</sup> However, the declining rate of pH and ultimately the final pH value varied with different amino acids and initiator concentration. Final pH was found within 2.5 to 4.5, which is required for free radical polymerization reaction.<sup>9,17</sup> The maintenance of pH could be explained by the

**Table I.** g-Factor, Band Gap, and Conductivity of Chiral Polyaniline

Polymer	APS (mol)	Dissymmetry g-factor $\times 10^{-2}$	Band gap (eV)	Conductivity (S cm <sup>-1</sup> ) $\times 10^{-1}$
(L)-Ile.PANI	0.05	-0.060	1.80, 2.67, 4.24	4.1
	0.1	-0.017	1.99, 4.47	5.8
(L)-Leu.PANI	0.05	-0.056	2.08, 4.39	5.7
	0.1	-0.047	2.38, 2.95, 4.68	6.7
(L)-Phe.PANI	0.05	-0.071	2.25, 4.68	7.8
	0.1	-0.039	2.28, 3.96, 4.22	7.2

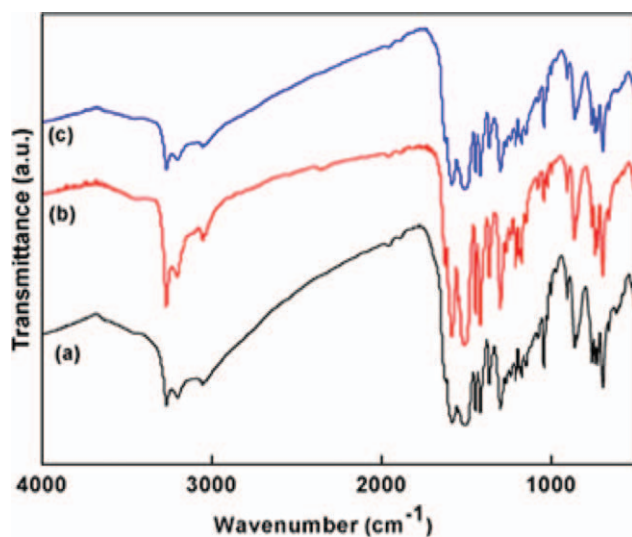


**Figure 2.** FTIR spectra of (a) (L)-Ile.PANI, (b) (L)-Leu.PANI, and (c) (L)-Phe.PANI. [Color figure can be viewed in the online issue, which is available at [wileyonlinelibrary.com](http://wileyonlinelibrary.com).]

amido group in amino acids that neutralizes the produced  $H^+$  during the polymerization. Therefore, the saturated solution acts as a buffer solution, and it controls the pH value during the polymerization.

It seems that the formation of these specific morphologies depends on two different mechanisms. When APS is 0.05M in concentration, there are plenty of aniline monomers in the solution due to high concentration, hence the oxidation of the aniline monomers tends to form phenazine structure and yield oligomers in the initial weak acid ( $pH \sim 4.4$ ) solution.<sup>17</sup> The morphology of these oligomers is usually in the lamellar shape and may act as a secondary soft template for PANI growth.<sup>15–19</sup> Therefore, PANI of the flaky morphology forms in this condition. However, in other cases (0.1M APS), aniline monomers form a complex with amino acids by hydrogen bonding. These complexes usually form fibers or flaky fibers by self-assembly<sup>20</sup> and thus acting as the template for the formation of PANI fibers and helix. Moreover, the pH value of this solution is above 2.6, which prevents the other morphologies formation during the polymerization and fasten the intrinsic one-dimensional growth in solution.

Figure 4 shows the UV-vis spectra of chiral PANI, which is dissolved in chloroform. The strong peak at 265 nm is ascribed to the  $\pi-\pi^*$  transition in the substituted phenazine, which forms during aniline oxidation in the buffer solution. The very weak absorption band centered at 520 nm is attributed to the  $n-\pi^*$  transition in the substituted phenazine.<sup>21</sup> At higher (optimum) initiator concentration, a weak absorption band at 303 nm was found. This band is mainly because of the protonation which leads to the phase segregation of unprotonated and fully protonated domains, followed by a transition from isolated, doubly charged, spinless, bipolaron to polaronic metal.<sup>22</sup> Due to phase segregation, different band gap (values are for the different phase segregation obtained from UV-vis spectra) values are obtained because at initial stage of oxidation, the branching

structure caused by the presence of phenazine units in polymer chain stabilizes different charge state in polymer by more protonation of quinoid form. It is shown in Supporting Information Figure S3 that the band gap (Tauc's plot) of chiral PANI obtained by higher initiator ratio is more than that of lower initiator ratio. These band gap results are in well agreement with conductivity data obtained from four probe method and justify the above hypothesis.

The observed doping ratio is (L)-Phe.PANI > (L)-Leu.PANI > (L)-Ile.PANI. The low doping ratio means that a few PANI main chains are protonated. When the pH value of solution is higher than 2.0, there are both anilinium cations and neutral aniline molecules in the solution.

Therefore, there are two kinds of polymerization process of aniline, one is forming oligomers having mixed ortho- and para coupled aniline constitutional units and the other is forming protonated PANI by adding anilinium cations in para position. When pH value is above 4.4, the former process is dominated and vice versa.<sup>9</sup>

Further results were inferred by CD spectra and correlated with UV-vis spectroscopic data, which deal with chirality of the PANI chain. The negative ICD peak at 240 nm is ascribed to the  $\pi-\pi^*$  transition in the phenazine. The peaks at 325 as well as 420 nm are attributed to the  $\pi-\pi^*$  transition in the protonated structure of PANI chains. The weak ICD band around 680 nm is generated from the  $n-\pi^*$  transition in the phenazine. The features of CD spectra are in agreement with the UV-vis spectra. The ICD peak at 420 nm is the characteristic peak of helical conformation or helical packing of PANI chains<sup>23</sup> so the chirality of PANI can be estimated by evaluating Figure 4. The CD spectra show relatively weak bisignate (split) cotton effect with almost zero crossing centered at the polymer chains  $\pi-\pi^*$  transition (around 420 nm in the UV-vis spectra). Such bisignate cotton effects are expected from exciton coupling between

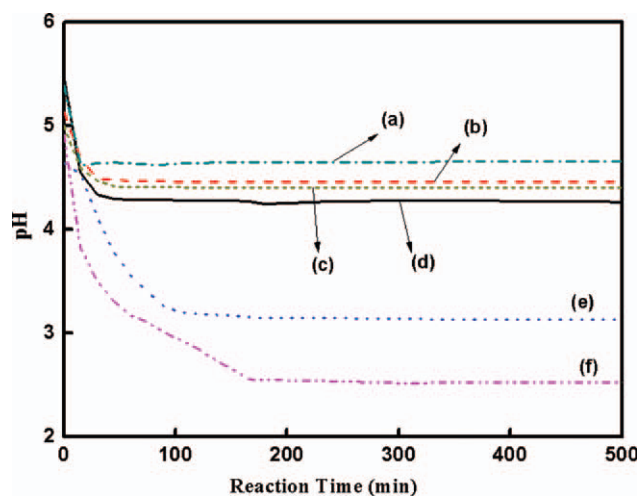


**Figure 3.** Variation in pH values against reaction time at 0.05M APS for (a) (L)-Ile.PANI, (b) (L)-Ile.PANI, and (c) (L)-Phe.PANI, and 0.1MAPS for (d) (L)-Ile.PANI, (e) (L)-Ile.PANI, and (f) (L)-Phe.PANI. [Color figure can be viewed in the online issue, which is available at [wileyonlinelibrary.com](http://wileyonlinelibrary.com).]

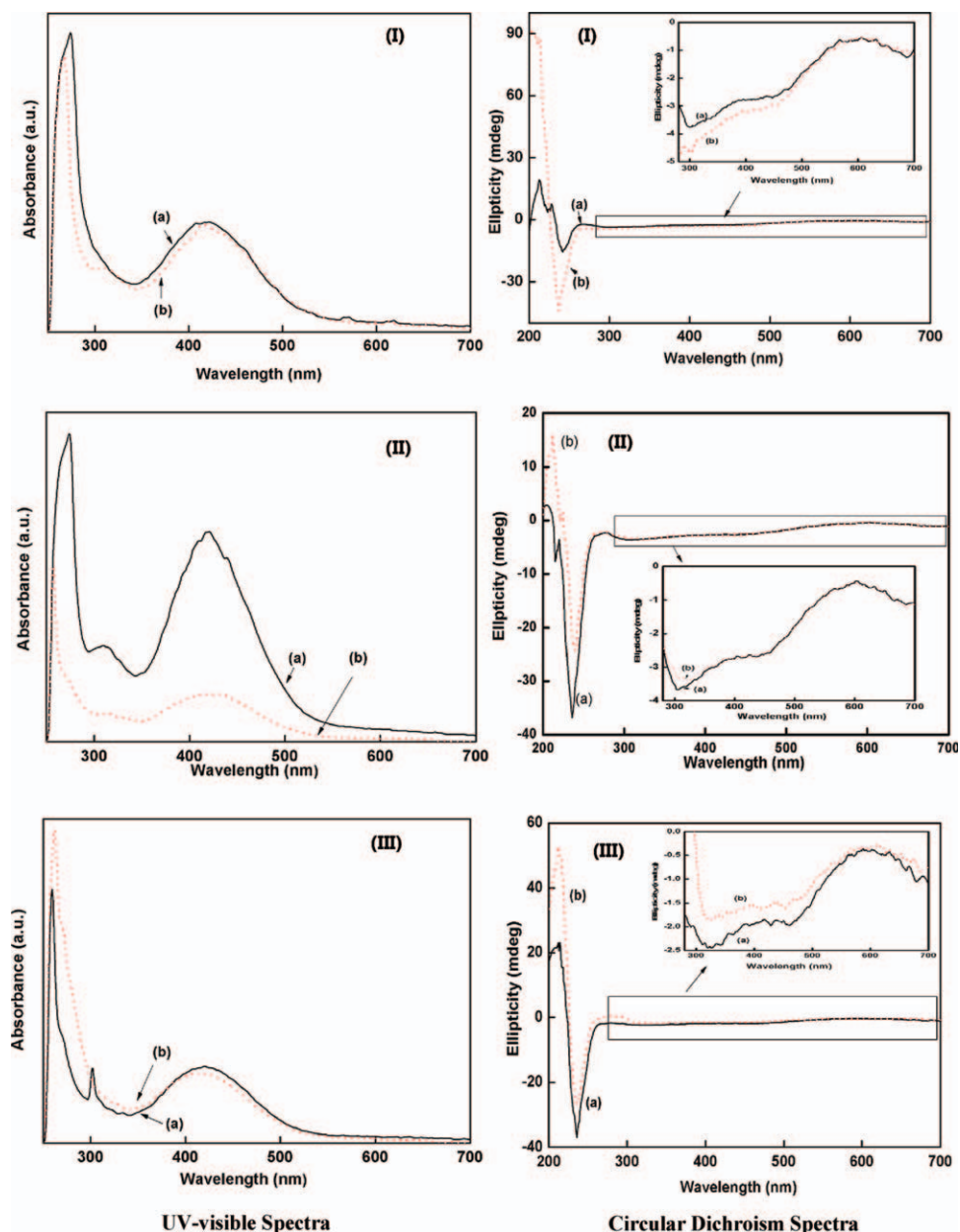


**Figure 4.** UV-vis and CD spectra of chiral PANI; (I) (L)-Ile.PANI, (II) (L)-Ieu.PANI, and (III) (L)-Phe.PANI; Solid line and dotted line for 0.05M and 0.1M APS, respectively. [Color figure can be viewed in the online issue, which is available at [wileyonlinelibrary.com](http://wileyonlinelibrary.com).]

obliquely oriented neighboring transition dipole moments suggesting that the polymer chains were aggregated in a chiral organization.<sup>13</sup> These results are further supported by dissymmetry  $g$ -factor [ $CD/(Absorbance/32980)$ ]. The trend of  $g$ -factor absolute values are demonstrated in Table I, which shows that the  $g$ -factor decreases with increase in molar ratio of initiator. So, it is clear that the reaction proceeds with the highest stereoselectivity at lower concentration of initiator.<sup>24,25</sup>

## CONCLUSIONS

This work has demonstrated the new super-structural morphology of PANI with phase segregation, which have been created using a naturally occurring chiral amino acids as soft template

through the electrostatic interaction and hydrogen bonding between PANI and amino acids. The branched structure caused by the presence of phenazine units in polymer chain stabilizes different charge state in polymer with a higher conductivity. We believe that the results shown here would open a way to obtain novel chiral conducting polymer superstructures at large scale with known morphology and better conductivity.

## ACKNOWLEDGMENTS

The authors thank Prof. P. B. Sharma, Vice-Chancellor, Delhi Technological University (formerly Delhi College of Engineering), Delhi for encouragement and support. Sudha thanks DTU, Delhi for financial support. The authors also thank

DST, New Delhi for the financial assistance under DST-JSPS collaborative research project.

## REFERENCES

1. Huang, J.; Virji, S.; Weiller, B. H.; Kaner, R. B. *J. Am. Chem. Soc.* **2003**, *125*, 314.
2. Marinakos, S. M.; Anderson, M. F.; Ryan, J. A.; Martin, L. D.; Felheim, D. L. *J. Phys. Chem. B* **2001**, *105*, 8872.
3. Liang, L.; Liu, J.; Windish, C. F.; Exarhos, G. J.; Lin, Y. *Angew. Chem. Int. Ed. Engl.* **2002**, *41*, 3665.
4. Li, C.; Hatano, T.; Takeuchi, M.; Shinkai, S. *Chem. Commun.* **2004**, 2350.
5. Dmitrieva, E.; Dunsch, L. *J. Phys. Chem. B* **2011**, *115*, 6401.
6. Goto, H.; Akagi, K. *Angew. Chem. Int. Ed. Engl.* **2005**, *44*, 4322.
7. Huang, J.; Kaner, R. B. *Angew. Chem. Int. Ed. Engl.* **2004**, *43*, 5817.
8. Venancio, E. C.; Wang, P.; MacDiarmid, A. G. *Synth. Met.* **2006**, *156*, 357.
9. Stejskal, J.; Sapurina, I.; Trchová, M.; Konyushenko, E. N. *Macromolecules* **2008**, *41*, 3530.
10. Elsayed, A. H.; Eldin, M. S. M.; Elsyed, A. M.; Elazm, A. H. A.; Younes, E. M.; Motaweh, H. A. *Int. J. Electrochem. Sci.* **2011**, *6*, 206.
11. Stammer, C.; Taurins, A. *Spectrochim. Acta* **1963**, *19*, 1625.
12. Mitchell, M. B.; Smith, G. R.; Guillory, W. A. *J. Chem. Phys.* **1981**, *75*, 44.
13. Satrijo, A.; Meskers, S. C. J.; Swager, T. M. *J. Am. Chem. Soc.* **2006**, *128*, 9030.
14. Ping, Z. *J. Chem. Soc. Faraday Trans.* **1996**, *92*, 3063.
15. Sapurina, I.; Stejskal, J. *Polym. Int.* **2008**, *57*, 1295.
16. Konyushenko, E. N.; Stejskal, J.; Sedenkova, I.; Trchova, M.; Sapurina, I.; Cieslar, M.; Prokes, J. *Polym. Int.* **2006**, *55*, 31.
17. Zhang, L.; Zhang, L.; Wan, M. *Eur. Polym. J.* **2008**, *44*, 2040.
18. Andriotis, A. N.; Menon, M.; Srivastava, D.; Chernozatonskii, L. *Phys. Rev. Lett.* **2001**, *87*, 066802.
19. Zhang, L.; Zujovic, Z. A.; Peng, H.; Bowmaker, G. A.; Kilmartin, P. A.; Travas-Sejdic, J. *Macromolecules* **2008**, *41*, 8877.
20. Zhang, L.; Wan, M. *Adv. Funct. Mater.* **2003**, *13*, 815.
21. Venancio, E. C.; Wang, P.; MacDiarmid, A. G. *Synth. Met.* **2006**, *156*, 357.
22. Guo, H.; Knobler, C. M.; Kaner, R. B. *Synth. Met.* **1999**, *101*, 44.
23. Li, W.; Wang, H. L. *J. Am. Chem. Soc.* **2004**, *126*, 2278.
24. Zhang, X.; Song, W.; Harris, P. J. F.; Mitchell, G. R. *Chem. Phys. Chem.* **2007**, *8*, 1766.
25. Yang, Y.; Chen, S.; Xu, L. *Macromol. Rapid Commun.* **2011**, *32*, 593.